

## 1. Experimental Materials

### 1.1 Reagents and Chemicals

All chemicals and reagents were of analytical grade and used without further purification unless specified. 4-((4-(Pyridin-3-yl) pyrimidin-2-ylamino) methyl) benzoic acid (MGC),  $\text{CoCl}_2 \cdot 6\text{H}_2\text{O}$ ,  $\text{NiCl}_2 \cdot 6\text{H}_2\text{O}$ , and N,N-dimethylformamide (DMF) were purchased from Sinochem Pharmaceuticals. Human pancreatic cancer cells (BxPC-3) were obtained from Procell Life Science & Technology Co., Ltd. (Wuhan, China). FITC and propidium iodide (PI) were sourced from BD Biosciences. Plasmid pBR322 DNA and calf thymus DNA (CT-DNA) were acquired from Sigma-Aldrich. Staining buffer, RNase A, and PI were supplied by Biosharp.

### 1.2 Cell Culture

Incubate BxPC-3, Panc-1, L929 cells in a humidified incubator at 37°C with 5%  $\text{CO}_2$ . cells were cultured in RPMI 1640 or DMEM medium, supplemented with fetal bovine serum (FBS), streptomycin, and penicillin.

### 1.3 ROS Scavenging Assay

BxPC-3 cells were stained with 2,7-dichlorodihydrofluorescein diacetate (DCFH-DA, Sigma-Aldrich). Cells ( $5 \times 10^3$ ) from culture dishes were treated with 10 mM N-acetyl-L-cysteine (NAC), followed by co-treatment with 50  $\mu\text{M}$  Co-MGC or 50  $\mu\text{M}$  Ni-MGC for 24 h. Subsequently, the culture medium was aspirated, and the cells were washed with ice-cold phosphate-buffered saline (PBS, 1X). The cells were then detached using EDTA-free trypsin and centrifuged at 1500 rpm for 4 minutes. After two washes with PBS, the cell pellet was resuspended in 100  $\mu\text{L}$  of binding buffer. Next, 5  $\mu\text{L}$  of Annexin V-FITC and 5  $\mu\text{L}$  of propidium iodide (PI) were added, followed by incubation in the dark for 15 minutes. Finally, 400  $\mu\text{L}$  of binding buffer was added, and the samples were filtered and analyzed using an Accuri C6 flow cytometer.

## 2. Crystallographic Data

**Tab. S1** Crystallographic data for Co-MGC and Ni-MGC.

Empirical formula	$\mathbf{C_{37}H_{37}CoN_9O_7}$
Formula weight	778.68
Temperature/K	300.15
Crystal system	monoclinic
Space group	Pc
$a/\text{\AA}$	14.0516(5)
$b/\text{\AA}$	6.7554(2)
$c/\text{\AA}$	20.0211(7)
$\alpha/^\circ$	90
$\beta/^\circ$	108.084(4)
$\gamma/^\circ$	90
Volume/ $\text{\AA}^3$	1806.61(11)
$Z$	2
$\rho_{\text{calc}}/\text{cm}^3$	1.431
$\mu/\text{mm}^{-1}$	4.255
$F(000)$	810.0
Radiation	$\text{CuK}\alpha (\lambda = 1.54184)$
$2\Theta$ range for data collection/°	9.294 to 159.652
Index ranges	$-16 \leq h \leq 15, -7 \leq k \leq 5, -24 \leq l \leq 24$
Reflections collected	8820
Independent reflections	4391 [ $R_{\text{int}} = 0.0274, R_{\text{sigma}} = 0.0355$ ]
Data/restraints/parameters	4391/14/469
Goodness-of-fit on $F^2$	1.137
Final R indexes [ $I \geq 2\sigma (I)$ ]	$R_1 = 0.0476, wR_2 = 0.1197$
Final R indexes [all data]	$R_1 = 0.0612, wR_2 = 0.1593$
Largest diff. peak/hole / e $\text{\AA}^{-3}$	0.70/-0.83
Flack parameter	0.384(10)

Empirical formula	$\mathbf{C_{34}H_{32}N_8NiO_6}$
Formula weight	707.38
Temperature/K	299.15
Crystal system	monoclinic
Space group	Pc
$a/\text{\AA}$	13.93393(16)
$b/\text{\AA}$	6.73940(6)
$c/\text{\AA}$	20.0825(2)
$\alpha/^\circ$	90

$\beta/^\circ$	107.9299(13)
$\gamma/^\circ$	90
Volume/ $\text{\AA}^3$	1794.29(4)
Z	2
$\rho_{\text{calc}} \text{g/cm}^3$	1.309
$\mu/\text{mm}^{-1}$	1.231
F(000)	736.0
Radiation	$\text{CuK}\alpha (\lambda = 1.54184)$
2 $\Theta$ range for data collection/°	6.668 to 136.384
Index ranges	$-16 \leq h \leq 16, -7 \leq k \leq 8, -23 \leq l \leq 23$
Reflections collected	8660
Independent reflections	8660 [ $R_{\text{int}} = ?, R_{\text{sigma}} = 0.0375$ ]
Data/restraints/parameters	8660/11/460
Goodness-of-fit on $F^2$	1.057
Final R indexes [ $I \geq 2\sigma (I)$ ]	$R_1 = 0.0439, wR_2 = 0.1228$
Final R indexes [all data]	$R_1 = 0.0445, wR_2 = 0.1236$
Largest diff. peak/hole / e $\text{\AA}^{-3}$	0.42/-0.47
Flack parameter	0.62(3)

**Tab. S2** The fractional bonding length of Co-MGC and Ni-MGC.

Atom	Atom	Length/ $\text{\AA}$
Co01	O002	2.140(6)
Co01	O003	2.071(8)
Co01	O005	2.175(6)
Co01	N007 <sup>1</sup>	2.180(7)
Co01	O00A	2.048(8)
Co01	N00I <sup>2</sup>	2.180(8)

<sup>1</sup>+X,2-Y,-1/2+Z; <sup>2</sup>+X,-Y,1/2+Z

Atom	Atom	Length/ $\text{\AA}$
Ni1	O24	2.059(4)
Ni1	O47	2.046(4)
Ni1	O48	2.121(4)
Ni1	N8	2.115(4)
Ni1	O49	2.090(4)
Ni1	N31	2.123(4)

<sup>1</sup>+X,2-Y,1/2+Z; <sup>2</sup>+X,-Y,-1/2+Z

**Tab. S3** The selected bond angles of Co-MGC and Ni-MGC.

<b>Atom Atom Atom</b>	<b>Angle/°</b>	<b>Atom Atom Atom</b>	<b>Angle/°</b>
O002 Co01 O005	173.4(3)	O005 Co01 N007 <sup>1</sup>	91.7(3)
O002 Co01 N007 <sup>1</sup>	93.9(3)	O005 Co01 N00I <sup>2</sup>	88.8(3)
O002 Co01 N00I <sup>2</sup>	85.6(3)	O00A Co01 O002	91.9(3)
O003 Co01 O002	90.8(3)	O00A Co01 O003	177.3(3)
O003 Co01 O005	93.0(3)	O00A Co01 O005	84.3(3)
O003 Co01 N007 <sup>1</sup>	86.8(3)	O00A Co01 N007 <sup>1</sup>	93.0(3)
O003 Co01 N00I <sup>2</sup>	92.2(3)	O00A Co01 N00I <sup>2</sup>	88.0(3)

<b>Atom Atom Atom</b>	<b>Angle/°</b>	<b>Atom Atom Atom</b>	<b>Angle/°</b>
C22 O24 Ni1	127.3(4)	C9 N8 Ni1	120.3(3)
C45 O47 Ni1	126.1(4)	C32 N31 Ni1	121.6(4)
C13 N8 Ni1	121.4(4)	C36 N31 Ni1	120.9(4)

### 3. Supplementary Experimental Data

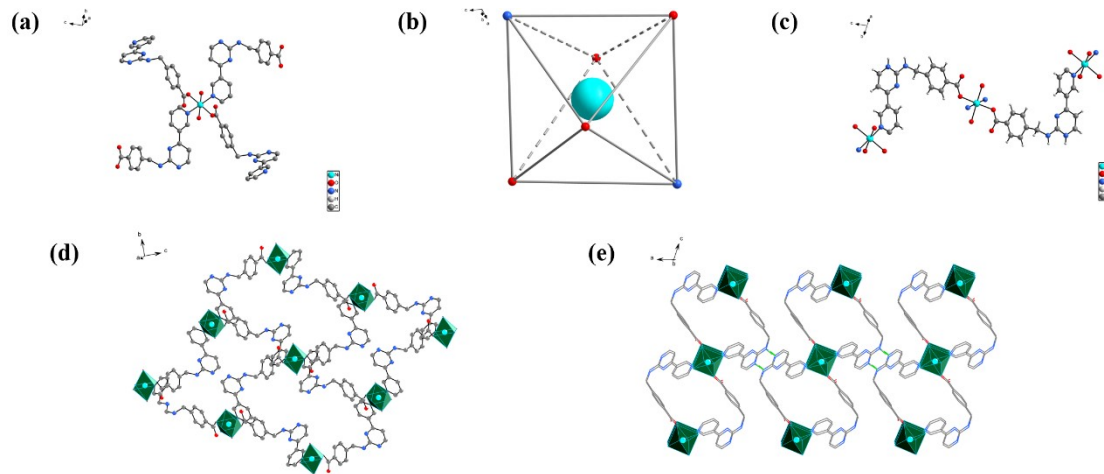


Fig. S1. Single - crystal structure of Ni - MGC (C, gray; O, red; N, deep blue; Ni, sky blue; all hydrogen atoms are omitted for clarity): (a) Coordination environment of Ni; (b) Symmetrical unit of Ni - MGC; (c) Coordination mode of ligand; (d) 2D structure; (e) 3D structure.

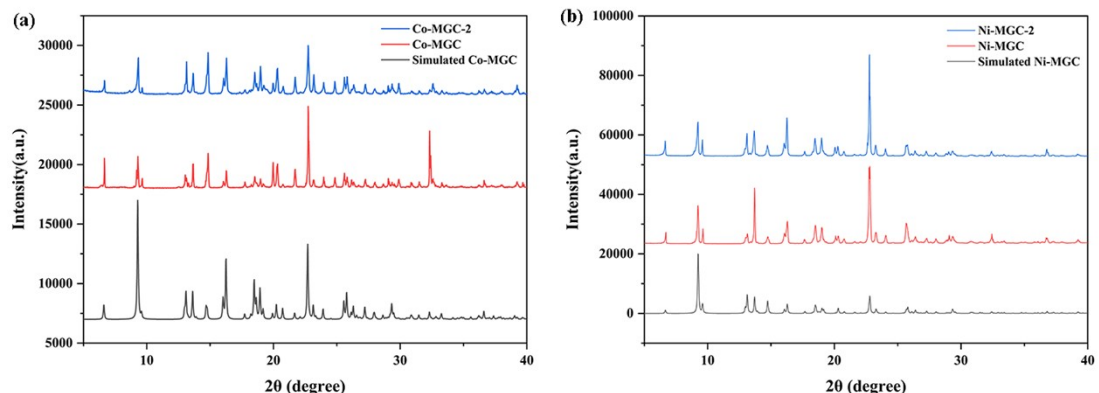


Fig. S2. XRD patterns of different batches of Co-MGC and Ni-MGC

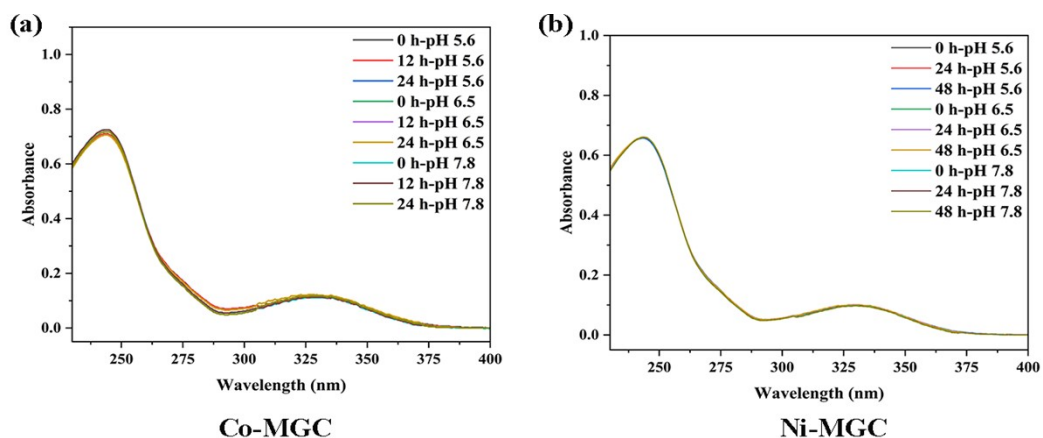


Fig. S3. (a) and (b) Stability of Co-MGC and Ni-MGC in buffer solutions at pH 7.4, pH 6.5, and pH 5.6 at different time points (0h, 24h and 48h)

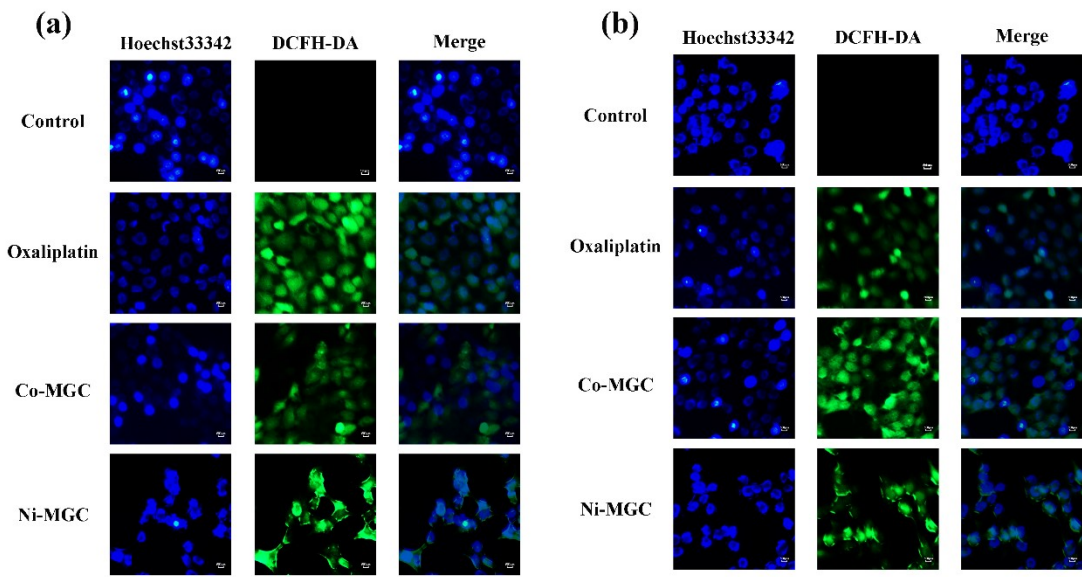


Fig. S4. Fluorescence imaging of ROS in BxPC - 3 cells (scale bar: 500  $\mu$ m): (a) Cycle 2; (b) Cycle 3.

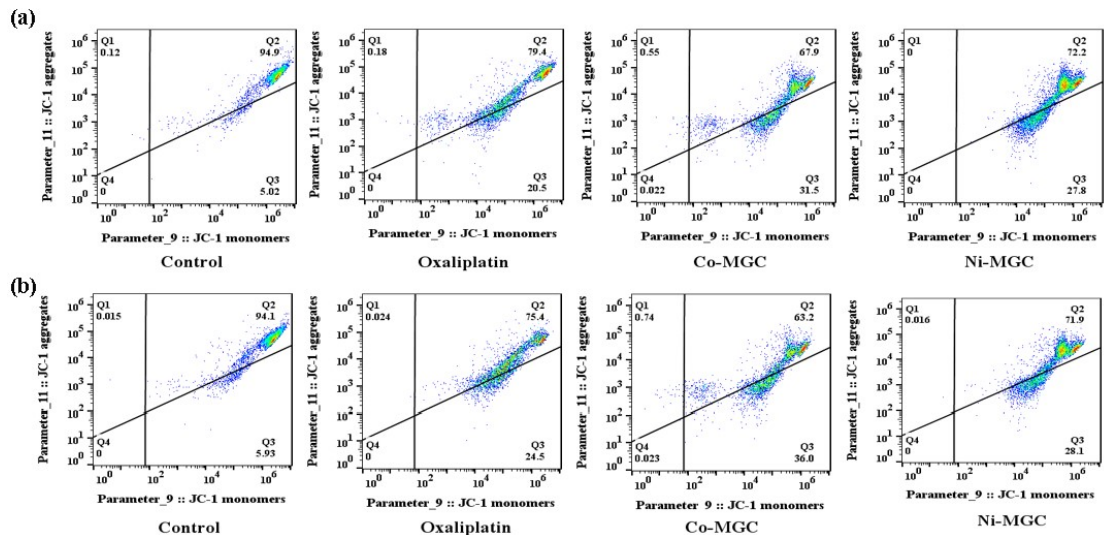


Fig. S5. JC-1 flow cytometry analysis of mitochondrial membrane potential ( $\Delta\Psi_m$ ). Membrane potential detection in untreated cells, cells treated with oxaliplatin (50  $\mu$ M), Co-MGC (50  $\mu$ M), or Ni-MGC (50  $\mu$ M) for 24 hours: (a) Cycle 2; (b) Cycle 3.

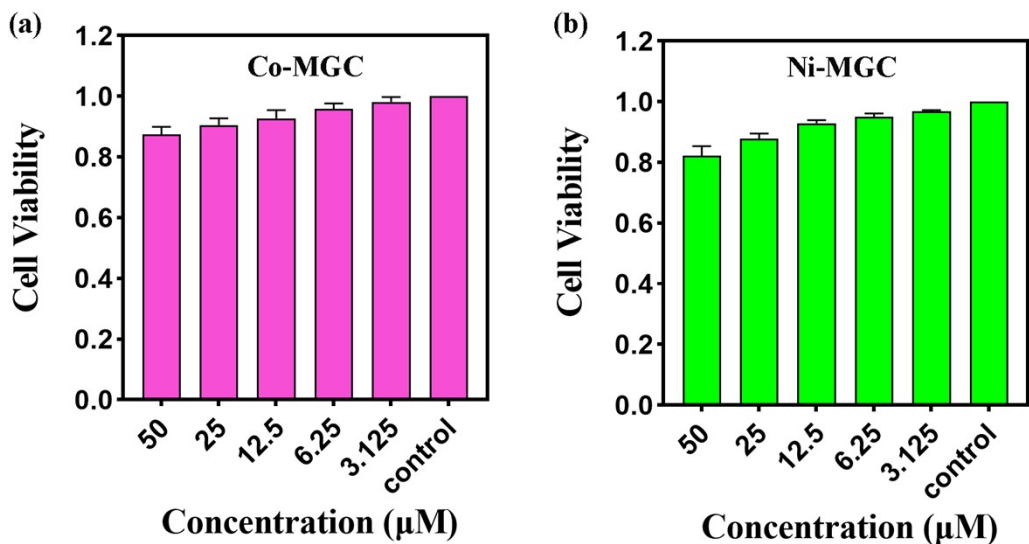


Fig. S6. Schematic diagram of cytotoxicity of Co-MGC and Ni-MGC on L929 cells

Tab. S4. Cytotoxicity of Co-MGC, Ni-MGC, in BxPC-3 and Panc-1 cells.

Complex	BxPC-3[IC <sub>50</sub> ( $\mu\text{M}$ )]	Panc-1[IC <sub>50</sub> ( $\mu\text{M}$ )]
Co-MGC	8.28 $\pm$ 2.32	37.98 $\pm$ 6.76
Ni-MGC	10.23 $\pm$ 2.89	58.2 $\pm$ 13.64

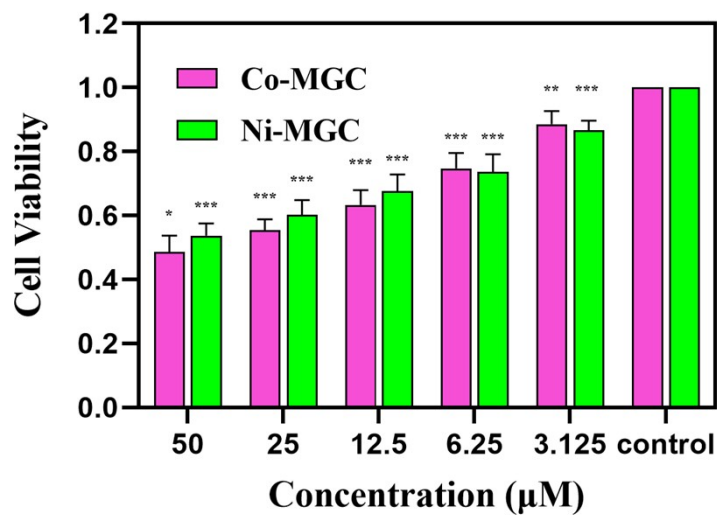


Fig. S7. Schematic diagram of cytotoxicity of Co MGC and Ni MGC on Panc-1 cells Values

are expressed as mean  $\pm$  SD. \*p < 0.05, \*\*p < 0.01, \*\*\*p < 0.001.

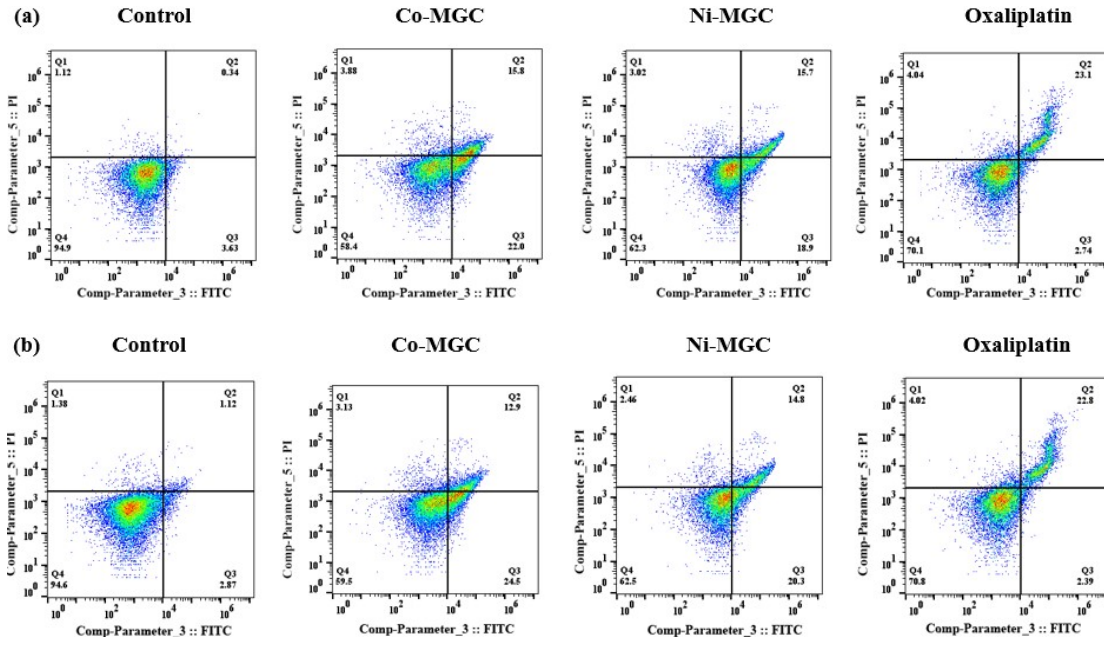


Fig. S8. Apoptosis induction in BxPC-3 cells after 24-hour incubation with Co-MGC, Ni-MGC, and Oxaliplatin: (a) Cycle 2; (b) Cycle 3.

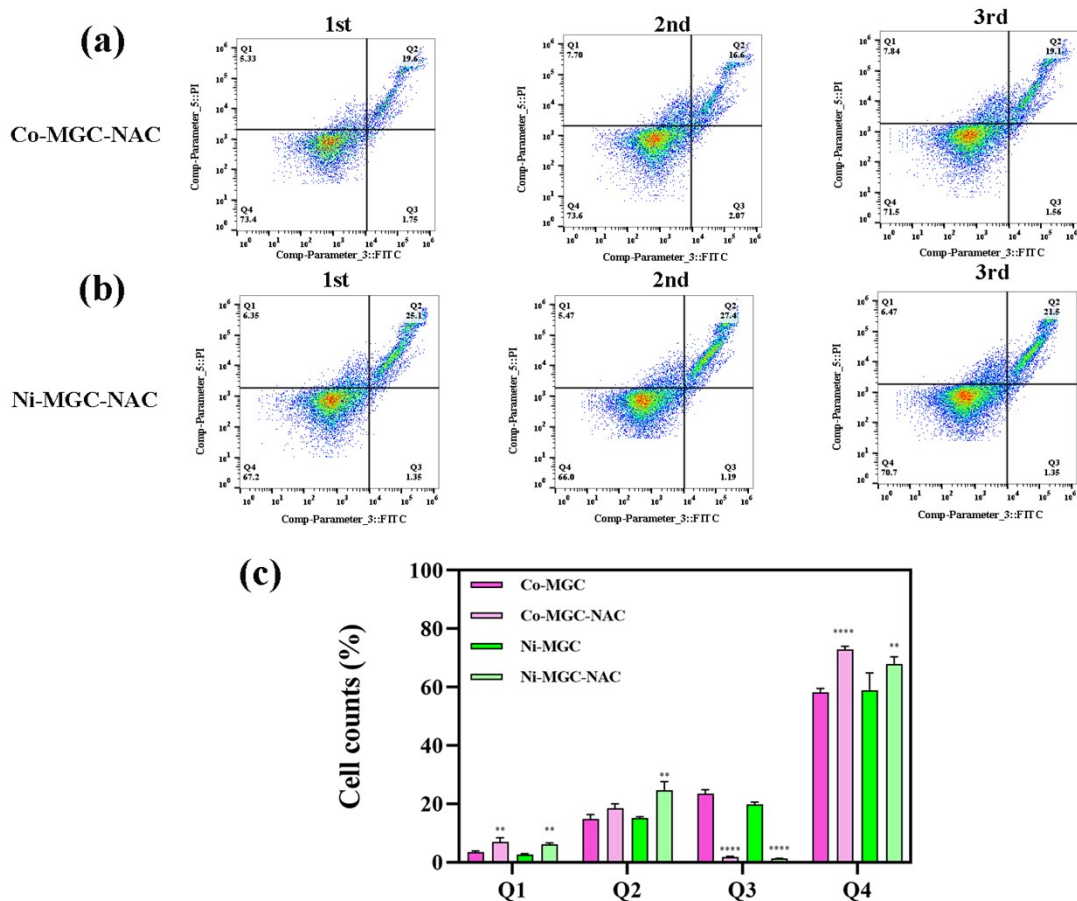


Fig. S9. Apoptosis and cell cycle distribution of BxPC-3 cells after co incubation with Co MGC, Ni MGC, and NAC for 24 hours. Values are expressed as mean  $\pm$  SD. \*p < 0.05, \*\*p < 0.01, \*\*\*p < 0.001.

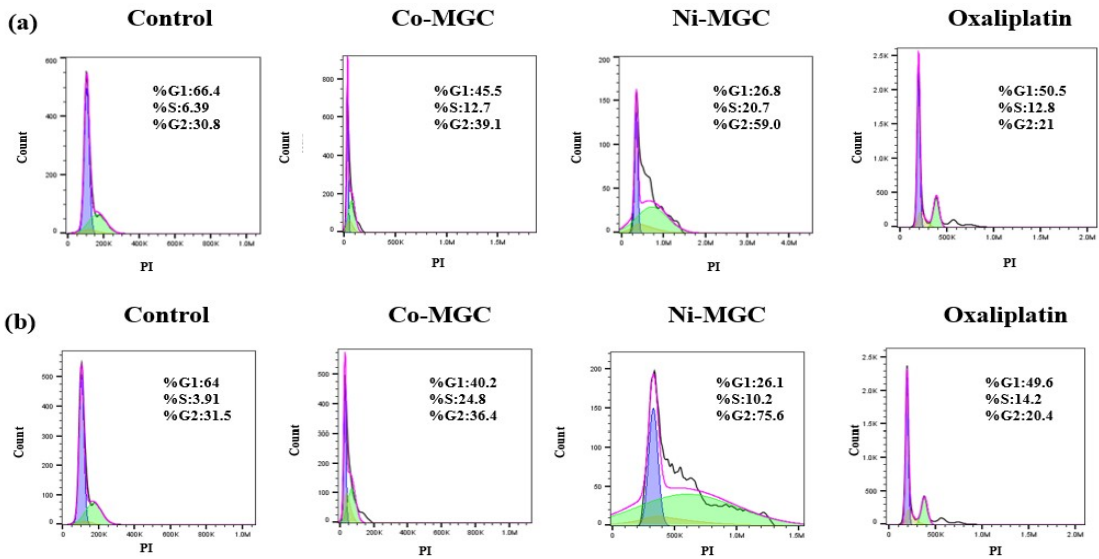


Fig. S10. Cell cycle distribution in BxPC-3 cells after 24-hour incubation with Co-MGC, Ni-MGC, and Oxaliplatin: (a) Cycle 2; (b) Cycle 3.

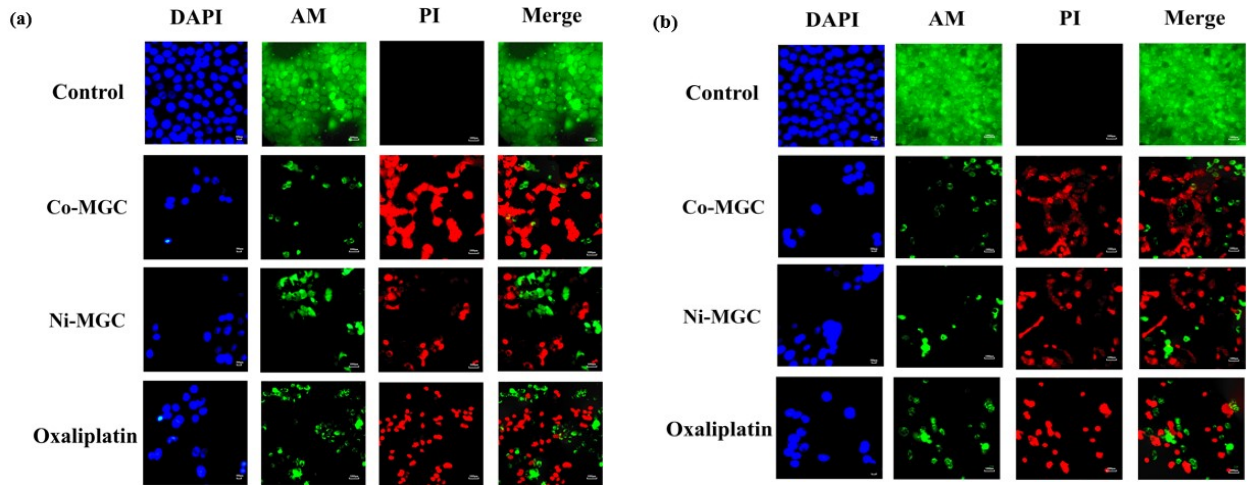


Fig. S11. Fluorescence images of BxPC-3 cells stained with DAPI (scale bar: 500  $\mu$ m) and AM/PI co-staining images (scale bar: 1000  $\mu$ m) following different treatments: (a) Cycle 2; (b) Cycle 3.